JAIST Repository
https://dspace.jaist.ac.jp/

| | |
|---|---|
| Title | Molecular Design of Polyampholytes for Vitrification-Induced Preservation of Three-Dimensional Cell Constructs without Using Liquid Nitrogen |
| Author(s) | Matsumura, Kazuaki; Hatakeyama, Sho; Naka, Toshiaki; Ueda, Hiroshi; Rajan, Robin; Tanaka, Daisuke; Hyon, Suong-Hyu |
| Citation | Biomacromolecules, 21(8): 3017-3025 |
| Issue Date | 2020-07-13 |
| Type | Journal Article |
| Text version | publisher |
| URL | http://hdl.handle.net/10119/17577 |
| Rights | This is an open access article published under an ACS AuthorChoice License (https://acsopenscience.org/open-access/licensing-options/), which permits copying and redistribution of the article or any adaptations for non-commercial purposes. Kazuaki Matsumura, Sho Hatakeyama, Toshiaki Naka, Hiroshi Ueda, Robin Rajan, Daisuke Tanaka, and Suong-Hyu Hyon, Biomacromolecules, 2020, 21(8), pp.3017-3025. DOI:10.1021/acs.biomac.0c00293 |
| Description | |

JAIST
JAPAN
ADVANCED INSTITUTE OF
SCIENCE AND TECHNOLOGY

Japan Advanced Institute of Science and Technology

This is an open access article published under a Creative Commons Non-Commercial No Derivative Works (CC-BY-NC-ND) Attribution License, which permits copying and redistribution of the article, and creation of adaptations, all for non-commercial purposes.

ACS AUTHORCHOICE

BioMACROMOLECULES

pubs.acs.org/Biomac

Article

# Molecular Design of Polyampholytes for Vitrification-Induced Preservation of Three-Dimensional Cell Constructs without Using Liquid Nitrogen

Kazuaki Matsumura,* Sho Hatakeyama, Toshiaki Naka, Hiroshi Ueda, Robin Rajan, Daisuke Tanaka, and Suong-Hyu Hyon

Cite This: *Biomacromolecules* 2020, 21, 3017−3025

Read Online

ACCESS | Metrics & More | Article Recommendations | Supporting Information

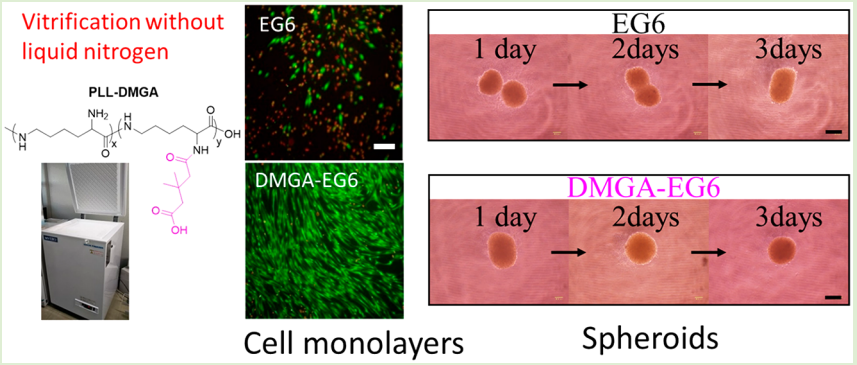


**ABSTRACT:** Current slow-freezing methods are too inefficient for cryopreservation of three-dimensional (3D) tissue constructs. Additionally, conventional vitrification methods use liquid nitrogen, which is inconvenient and increases the chance of cross-contamination. Herein, we have developed polyampholytes with various degrees of hydrophobicity and showed that they could successfully vitrify cell constructs including spheroids and cell monolayers without using liquid nitrogen. The polyampholytes prevented ice crystallization during both cooling and warming, demonstrating their potential to prevent freezing-induced damage. Monolayers and spheroids vitrified in the presence of polyampholytes yielded high viabilities post-thawing with monolayers vitrified with PLL-DMGA exhibiting more than 90% viability. Moreover, spheroids vitrified in the presence of polyampholytes retained their fusibilities, thus revealing the propensity of these polyampholytes to stabilize 3D cell constructs. This study is expected to open new avenues for the development of off-the-shelf tissue engineering constructs that can be prepared and preserved until needed.

## INTRODUCTION

Tissue engineering has emerged as a popular technology in the field of regenerative medicine with two- and three-dimensional (2D and 3D) regenerative tissues for the replacement of skin,[1] cartilage,[2] corneas,[3] blood vessels,[4] and retinas[5] having been reported. For tissue engineering to be industrialized, these tissue-cell constructs will require long-term storage before use. However, it is difficult to preserve the 2D or 3D structures of cell constructs during conventional slow freezing (at a cooling rate of 1 °C/min) because the ice crystals damage the junctions between the cells,[6] as well as nonuniform dehydration during freezing, and this causes lethal damage to the highly dehydrated areas of cells.[7] There are some studies that report the cryopreservation of 2D or 3D cell constructs through slow freezing;[8,9] however, this process is believed to have size limitations because the probable mechanism for reducing freezing damage relies on the inhibition of physical damage caused by the formation of intracellular and extracellular ice crystals.[10,11] For this reason, the cryopreservation of larger and more complicated cell constructs by the vitrification method has been studied.[12,13] Vitrification inhibits ice crystallization with water being solidified in a glassy state.[14] A recent study compared slow freezing and vitrification for the cryopreservation of tissue or cell constructs and found that vitrification was far superior for ovarian tissue preservation.[15]

Recently, the cryopreservation of 3D cell constructs by vitrification has garnered widespread attention for long-term storage and delivery.[16] Generally, high concentrations of solutes such as sucrose (Suc), ethylene glycol (EG), or dimethyl sulfoxide (DMSO) are required to inhibit crystal-

Received: February 28, 2020
Revised: July 10, 2020
Published: July 13, 2020

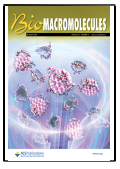

Downloaded via JAPAN ADVANCED INST SCIENCE TECHLGY on February 25, 2022 at 06:14:54 (UTC).
See https://pubs.acs.org/sharingguidelines for options on how to legitimately share published articles.

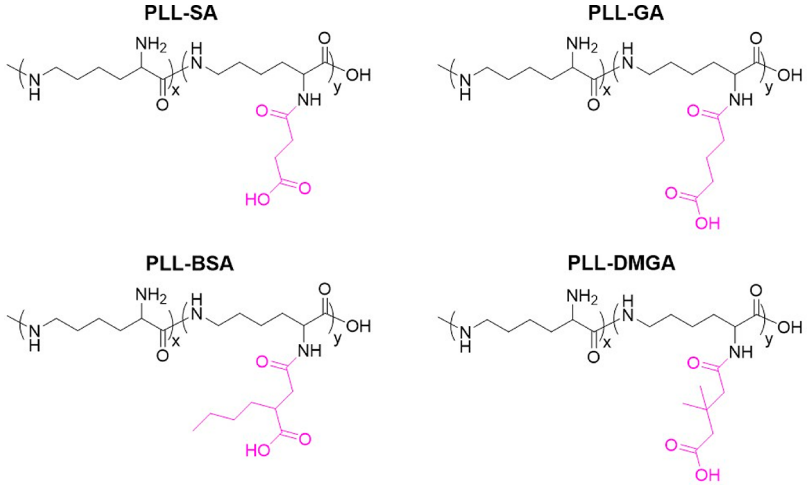


**Figure 1.** Chemical structures of various PLL-derived polyampholytes.

lization inside and outside of cells; however, this can be toxic for cells due to high osmotic pressure. Therefore, the development of novel methods of vitrification that have low toxicity and high efficiency is of paramount importance. Further, DMSO is expected to be replaced with other cryoprotectants (CPAs), especially in the field of regenerative medicine, because it has been reported to have an effect on the differentiation of stem cells.[17,18] However, little effort has been made to develop novel CPAs or stabilizers of the glassy state.

Recently, we reported that polyampholytes have high cryoprotective effects and low toxicities.[19−23] Carboxylated poly-L-lysine is an ampholytic polymer, having both positive and negative charges in the polymer chain, and exhibited better cryoprotective properties than DMSO. Furthermore, it had less influence on differentiation because it cannot penetrate the cell membranes.[19] Amphoteric polymers have also shown ice recrystallization inhibition.[24] Gibson has reported several macromolecular CPAs,[25,26] including polyampholytes, and suggested that the cryoprotective properties of polyampholytes were due to their inhibition of ice recrystallization.[27] In our previous studies using carboxylated poly-L-lysine, we developed a slow vitrification technique for 2D cell monolayers on liquid nitrogen vapor.[28−30] This technique requires no complicated procedures such as rapid cooling and warming due to the stabilization of the glassy state by the polyampholyte without the use of toxic cryoprotectants. However, 3D systems were not vitrified using this technique.

Vitrification in only 2D is insufficient for the large-scale development and industrialization of vitrification technology; 3D tissues and cell constructs should also be vitrified under the conditions used. Recently, spheroids have been used as building blocks for large scale tissue constructs such as blood vessels and cartilage.[31,32] If spheroids could be safely stored before use, the time required to prepare such tissues could be shortened considerably. Additionally, since the sizes of such spheroids are similar to those of embryos, it is believed that the vitrification technique could be extrapolated and successfully employed in reproductive medicine.[33,34] Furthermore, it is expected that the preparation of cell tissue constructs will be automated in the near future in order to standardize product quality in the industrial process. In such automated systems, the use of electric freezers would be far more productive than the use of liquid nitrogen. To this end, we aim to design polyampholytes capable of achieving the stable glassy state without the use of liquid nitrogen.

It has been reported that the introduction of hydrophobic moieties into molecules enhances ice recrystallization inhibition.[35,36] Therefore, in this study novel hydrophobic amphoteric polyelectrolytes were prepared and evaluated as vitrification stabilizing agents. Poly-L-lysine (PLL) was reacted with various carboxylic anhydrides to yield several ampholyte polymers that included hydrophobic moieties. The polymers were evaluated based on their ice crystallization inhibition abilities and mixed with EG, Suc, and ficoll to prepare vitrification solutions without DMSO. The crystallization behavior of each vitrification solution was monitored by differential scanning calorimetry (DSC). Moreover, the cytotoxicity of each amphoteric polymer was evaluated, and mesenchymal stromal cell (MSC) monolayers and spheroids were vitrified using these vitrification solutions at −150 °C in a freezer and their viabilities were evaluated.

## MATERIALS AND METHODS

**Preparation of Human MSC Monolayers and Spheroids.** Human bone marrow mesenchymal stromal cells (MSCs; HMS0047) established by Dr. Kato of Hiroshima University[37] were purchased from the RIKEN Cell Bank (RIKEN Bioresource Center, Ibaraki, Japan) in accordance with the regulations of the Life Science Committee of Japan Advanced Institute of Science and Technology. The cell culture was conducted with Dulbecco's modified Eagle's medium (DMEM; Sigma-Aldrich, St. Louis, MO, U.S.A.) containing 10% fetal bovine serum (FBS), 3 ng/mL of basic fibroblast growth factor (Wako Pure Chemical Industries Ltd., Osaka, Japan), 100 U/mL of penicillin, and 100 μg/mL of streptomycin at 37 °C under 5% $CO_2$ in a humidified atmosphere. The expanded cells were detached using 0.25% (w/v) trypsin containing 0.02% (w/v) ethylenediaminetetraacetic acid in phosphate-buffered saline without calcium or magnesium (PBS(−)) and were seeded on a new tissue culture plate for subculturing. The MSCs used in this study were between passages three and five. Two-dimensional cell monolayers were prepared by culturing MSC ($1.0 \times 10^5$/ mL) in a 3.5 cm dish for 7 days. Three-dimensional spheroids were prepared by placing the cell suspension ($1.0 \times 10^4$/100 μL) in a noncell-adhesive 96-well plate (PrimeSurface; Sumitomo Bakelite, Tokyo, Japan) that inhibited cell adhesion and culturing for 1 day.

**Synthesis of Amphoteric Polyelectrolyte.** Polyampholytes were synthesized using acid anhydrides and amines. In brief, a 25% (w/w) aqueous solution of ε-poly-L-lysine (PLL, JNC Corp., Tokyo, Japan) was reacted with different carboxylic anhydrides (succinic


https://dx.doi.org/10.1021/acs.biomac.0c00293
Biomacromolecules 2020, 21, 3017−3025

Table 1. Compositions of Various VSs and Their Abbreviations

| VS | polymers | concentration of polyampholytes/w/v % | EG/M | Suc/M | Ficoll/w/v % |
|---|---|---|---|---|---|
| EG5 | | 0 | 5 | 0.5 | 12.5 |
| EG6 | | 0 | 6 | 0.5 | 12.5 |
| SA-EG5 | PLL-SA | 10 | 5 | 0.5 | 12.5 |
| SA-EG6 | PLL-SA | 10 | 6 | 0.5 | 12.5 |
| GA-EG5 | PLL-GA | 10 | 5 | 0.5 | 12.5 |
| GA-EG6 | PLL-GA | 10 | 6 | 0.5 | 12.5 |
| BSA-EG5 | PLL-BSA | 10 | 5 | 0.5 | 12.5 |
| BSA-EG6 | PLL-BSA | 10 | 6 | 0.5 | 12.5 |
| DMGA-EG5 | PLL-DMGA | 10 | 5 | 0.5 | 12.5 |
| DMGA-EG6 | PLL-DMGA | 10 | 6 | 0.5 | 12.5 |
| PEG-EG5 | PEG | 10 | 5 | 0.5 | 12.5 |
| PEG-EG6 | PEG | 10 | 6 | 0.5 | 12.5 |

anhydride (SA), butyl succinic anhydride (BSA), glutaric anhydride (GA), and 3,3-dimethyl glutaric anhydride (DMGA); Wako Pure Chem. Ind. Ltd., Osaka Japan) at 65% molar ratios (anhydride/PLL amino groups) and 50 °C for 1−3 h to order to obtain the corresponding polyampholytes. The solutions were then neutralized by adding 5 M NaOH and lyophilized prior to use. The chemical structures were analyzed by $^1$H-nuclear magnetic resonance (NMR) spectroscopy (Bruker AVANCE III 400 MHz spectrometer, Bruker Biospin Inc., Switzerland) using $D_2O$ as the solvent. The spectra were analyzed using Topspin 3.6.1 software. Polyampholytes in this paper are denoted according to the anhydride used, such as PLL-SA, PLL-GA, PLL-BSA, and PLL-DMGA (Figure 1).

**Preparation of Vitrification Solutions (VSs).** We prepared VSs based on 5 or 6 M EG, 0.5 M Suc, and 12.5% (w/v) ficoll (GE Healthcare, Chicago, IL, U.S.A.) in PBS. PLL-SA, PLL-GA, PLL-BSA, PLL-DMGA, and polyethylene glycol (PEG, Mn = 20 000 Da) as a control were added to the solutions at 10% (w/v) to evaluate the effects of the polymers. The components of the various VSs are shown in Table 1, and their solution viscosities were determined using a rotating viscometer (TVE-22L, Toki Sangyo, Co., Ltd., Tokyo Japan). Equilibration solutions (ESs) consisting of 15% (v/v) EG in PBS and rewarming solutions (RSs) and dilution solutions (DSs) containing 1 and 0.5 M sucrose, respectively, were also prepared.

**Differential Scanning Calorimetry (DSC).** It is well understood that ice crystallization during cooling and heating should be inhibited during the vitrification process.[30] To analyze this, we thermally analyzed each VS using a differential scanning calorimeter (Q2000; TA Instruments, New Castle, DE, U.S.A.). Each solution (10 μL) was transferred to an aluminum pan and set on the calorimeter sample chamber. Measurements were collected by first cooling the pan to −170 °C at 10 °C/min, followed by warming to 40 °C at a heating rate of 10 °C/min.

**Ice Recrystallization Inhibition (IRI)-Cooling Splat Assay.** A modified splat assay was used to investigate the abilities of the polyampholytes to inhibit ice recrystallization during cooling.[38] The polymers were dissolved in PBS (pH 7.4), and the resulting solutions (20 μL) were dropped from a height of 1.5 m onto a glass coverslip, which was placed on a thin aluminum sheet on dry ice. This allowed the droplet to immediately form a thin wafer composed of very fine-grained ice with a diameter of 10−12 mm on the glass coverslip. After transferring the glass coverslip to a cryostage (Linkam Scientific), it was maintained at −6 °C. After 30 min of stabilization under a nitrogen atmosphere, microphotographs were taken using a Nikon DS Fi2 microscope fitted with crossed polarizers. ImageJ software (National Institutes of Health, Bethesda, MD) was used to analyze and process the images. The mean largest grain size (MLGS) obtained from five individual wafers was used to quantify the degree of recrystallization. The size was calculated relative to the size obtained with PBS buffer, which was used as the control sample.

**Vitrification of Cell Tissue Constructs without Liquid Nitrogen.** Schemes S1 and S2 show schematic illustrations of the vitrification processes for cell monolayers and spheroids. The cooling speed at −150 °C was determined by measuring the temperature of the monolayer and in the cryovial using thermocouples in two corners and the center of the freezer.

First, a 3.5 cm tissue culture dish covered with a confluent cell monolayer or centrifuged spheroids was immersed in 15% EG (ES) for a pre-equilibration period of 10 min, and then the ES was discarded. In the case of the vitrification of MSC monolayers, 2 mL of each VS was added on ice, and after 5 min the VS was removed by aspiration and the dish was placed in a −150 °C freezer. For spheroids, 200 μL of VS was added to the centrifuged spheroids, and after 5 min the suspension was transferred to a cryovial and put in the −150 °C freezer. After 1 week, the MSC monolayer was rapidly warmed by gently adding 2 mL of prewarmed RS. One minute later, RS was replaced with DS, and then after 3 min DMEM was used to wash the monolayer twice for 5 min. After cultured for 1 day in the incubator, staining of the recovered monolayers was performed with a fluorescence-based Live/Dead Assay Kit (Life Technologies, Carlsbad, CA, U.S.A.). This was followed by dispersing the cells using trypsin solution, and then the viability of the monolayers was evaluated using trypan blue staining. Viability was calculated using eq 1

$$\text{Viability}(\%) = \frac{\text{live cell}}{\text{live cell} + \text{dead cell}} \times 100 \quad (1)$$

When warming the spheroids, 2 mL of DMEM was first warmed and then directly introduced to the vial containing the vitrified spheroids, followed by washing twice with PBS for 5 min. Subsequent dissociation of the spheroids with collagenase (Wako, 125 Unit/mL) was conducted for 10 min, and the cell viabilities and recovery rates were evaluated with trypan blue staining. Additionally, cell viability was evaluated via spheroid fusibility immediately after thawing by placing spheroids in PrimeSurface96U multiwell plates and observing fusion for 3 days. Recovery rates were calculated using eq 2

$$\text{Recovery rate}(\%) = \frac{\text{live cell}}{\text{frozen cell}} \times 100 \quad (2)$$

To evaluate cell proliferation after vitrification of spheroids, live cells were dissociated and then seeded onto 24-well culture plates at a density of $2.5 \times 10^3/\text{cm}^2$ with 2 mL of DMEM ($n = 3$); the number of cells was counted over 1 week using Cell Counting Kit-8 (CCK-8, Dojindo, Kumamoto, Japan) following the supplier's instruction. Hematoxylin-Eosin (HE) staining of the frozen spheroid specimens was also evaluated just after warming.

**Cytotoxicity Assays.** The cytotoxicities of the various polyampholytes were evaluated by the 3-(4,5-dimethylthiazol-2-yl)-2,5-diphenyl tetrazolium bromide (MTT) method. MSCs suspended in 0.1 mL of medium at a concentration of $1.0 \times 10^4$ cells/mL were placed in a 96-well plate (Corning Inc., Corning, NY, USA). After incubation for 72 h at 37 °C, 0.1 mL of media containing different concentrations of polyampholyte solutions were added to the cells, followed by incubation for 48 h. The medium was then discarded, and the cells were rinsed three times with 0.2 mL of PBS. After this, 0.1


https://dx.doi.org/10.1021/acs.biomac.0c00293
Biomacromolecules 2020, 21, 3017−3025

mL of MTT solution (90 mg of MTT dissolved in 100 mL of the culture medium) was added, followed by incubation at 37 °C for 5 h. The insoluble formazan crystals formed by the reduction of MTT were dissolved in 0.1 mL of DMSO and their absorbances at 540 nm were recorded by a microplate reader (Versa Max, Molecular Device Japan K.K., Tokyo, Japan).

**Statistical Analysis.** All of the experiments were conducted in triplicate, and all of the data are expressed as the means ± standard deviations (SDs). When comparing data among more than three groups, the Tukey-Kramer test was used. Differences with $P$ values of less than 0.05 were considered statistically significant.

## RESULTS AND DISCUSSION

**Synthesis of Polyampholytes.** The NMR spectra of the polyampholytes (Figures S1−S4) clearly show that the desired polyampholytes were obtained with good purities. The results in Table 2 show the calculated degrees of substitution.

**Table 2. Degrees of COOH Substitution in Each Polyampholyte**

| polyampholytes | degree of substitution of COOH/% |
|---|---|
| PLL-SA | 64.8 ± 0.74 |
| PLL-GA | 63.8 ± 3.04 |
| PLL-BSA | 62.0 ± 3.30 |
| PLL-DMGA | 63.1 ± 0.21 |

**Stabilization of the Glassy State as Evaluated by DSC.** Thermal analysis of the various VSs was performed using DSC to evaluate the stabilization of the glassy state by the polyampholytes. We have previously reported the vitrification of human-induced pluripotent stem cells[39] and monolayers[30] by PLL-SA; however, we incorporated ficoll into VSs along with PLL-SA as ficoll has been extensively studied for vitrification owing to its stabilizing effect on the glassy state.[40,41] EG5 showed crystallization during cooling at −10 °C/min (Figure 2A), suggesting that 5 M of EG was not enough to inhibit ice crystallization, even in the presence of ficoll and Suc. However, using a 6 M solution of EG resulted in no crystallization during cooling, although devitrification through nucleation was observed during warming at around −90 °C (Figure 2B). Addition of polyampholytes or PEG containing 5 M EG resulted in inhibition of ice crystallization during freezing (Figure 2C,E,G,I,K); however, devitrification could still be observed during warming, indicating an inability to inhibit crystallization during warming. The nucleation temperature was lowest in PEG-EG5 (approximately −90 °C), then SA-EG5 (approximately −80 °C), and highest in DMGA-EG5 (approximately −50 °C), indicating that the glassy state stabilization abilities increased as follows: PEG < PLL-SA < PLL-GA < PLL-BSA < PLL-DMGA. A similar trend was observed in the DSC curves obtained when using 6 M EG. With PLL-SA, a devitrification peak was detected at −45 °C, and GA-EG6 showed a very small crystallization peak at −40 °C. Notably, BSA-EG6 and DMGA-EG6 did not show any crystallization peaks during either cooling or warming. On the basis of these results, BSA-EG6 and DMGA-EG6 can be used for slow vitrification at cooling and warming speed of 10 °C/min. This could be due to the enhancement of viscosity (Table S1) caused by molecular interactions when the hydrophobicity is increased,[42] which inhibits the molecular alignment required to form crystallites below the melting point. However, the devitrification temperature of SA-EG6 was much higher than that of PEG-EG6 even though they had similar viscosities, meaning that there could also be other mechanisms that inhibit nucleation that will require further study, such as the interactions of polyampholytes with water molecules.

Another interesting observation is that the glass transition temperature was found to be similar in all the VSs at temperatures in the range from −120 to −130 °C,[43] although a higher glass transition temperature was detected in DMGA-EG6. For storage or transportation of these vitrified tissue-cell constructs, the storage temperature should ideally be lower than the glass transition temperature to inhibit devitrification. Therefore, in this research a −150 °C electric freezer was tested for long-term storage without the use of liquid nitrogen.

**IRI Experiments.** Ice crystals are transformed into larger crystals during freezing and warming in a process known as recrystallization. To obtain better viability after vitrification, recrystallization should be avoided to reduce damage from intracellular and extracellular ice formation. To evaluate the ice recrystallization inhibition properties of each polyampholyte, we conducted IRI splat assays, and the results are shown in Figure 3. Compared with PBS, all polymer solutions had IRI activities at high concentrations of 10% (w/v). The IRI properties of PLL-BSA were the highest with an MLGS of around 32% with this increasing to 41%, 45%, 53%, and 58% for PLL-DMGA, PEG, PLL-GA, and PLL-SA, respectively. However, these values are not large compared to those seen for high IRI polymers such as poly(vinyl alcohol), which has a similar MLGS at a concentration of only 0.1%.[44] PEG is also included as a representative polymer that has lower IRI activity. These results combined with those obtained via DSC clearly suggest that the introduction of hydrophobic moieties to polyampholytes reduces the risk of devitrification of solutions by enhancing the stabilization of the glassy state rather than by inhibition of ice recrystallization.

**Slow Vitrification of MSC Monolayers at −150 °C.** The slow vitrification of MSC monolayers in a −150 °C freezer was examined. First, the cooling speed of cell suspensions in the freezer was investigated using thermocouple measurements at three points in the freezer (the center and two corners). The average cooling speed was 14.4 ± 0.40 °C/min (Figure S5); thus, the cooling speed in the freezer was higher than that used in the DSC measurements and slightly higher than that used in our previous study of slow vitrification using liquid nitrogen vapor (around 10 °C/min).[30] Successful vitrification of MSC monolayers should be achievable using polyampholytes under these conditions.

Figure 4A−F shows the results of live/dead assays after 1 day of warming with various VSs and 6 M EG. Figure 4A shows that when using an EG6 VS solution without a polymer, almost all of the cells were stained red, suggesting that they were dead and that devitrification during warming (Figure 2B) damaged the cell monolayer. Live/dead assays were conducted after thawing and then culturing for 1 day to reduce the overestimation of viability, as damaged cells can be mistakenly judged as alive immediately after thawing. The black spaces in Figure 4A,C,D indicate that damaged cells were detached from the dish. However, when PLL-SA was added into the VS (SA-EG6), almost all of the cells were alive after warming, and they were not detached from the dish (Figure 4B). This corresponds well with our previous results, which show the crystallization inhibition properties of PLL-SA.[24] In the case of warming by the addition of a prewarmed medium, it was also reported that the warming rate was much higher than 10 °C/min, so the risk of devitrification was low. PLL-DMGA was


https://dx.doi.org/10.1021/acs.biomac.0c00293
Biomacromolecules 2020, 21, 3017−3025

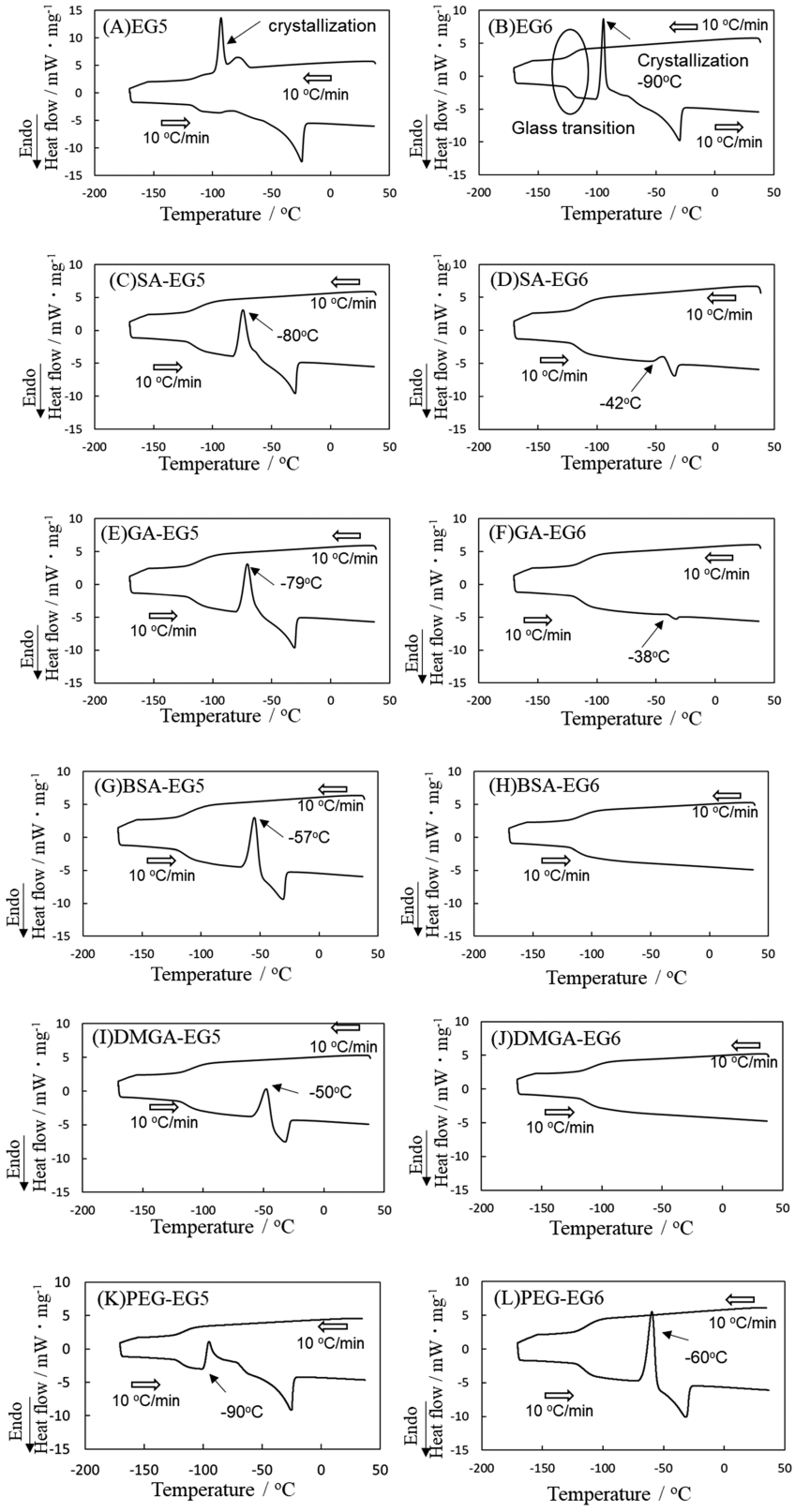


**Figure 2.** DSC thermograms of various VSs at cooling and heating rates of 10 °C/min. Peaks indicated by arrows represent crystallizations, while the shoulders at around −130 °C represent glass transitions.

found to enhance cell viability to the greatest extent (Figure 2E), which might be attributable to the inhibition of ice crystallization during both cooling and warming. A comparison of the viabilities when using the different VSs is shown in Figure 4G. DMGA-EG6 showed better viability than the PEG-EG6 control. Interestingly, GA-EG6 and BSA-EG6 resulted in significantly lower viabilities than SA-EG6 and DMGA-EG6 even though they showed the same lack of crystallization



https://dx.doi.org/10.1021/acs.biomac.0c00293
Biomacromolecules 2020, 21, 3017−3025

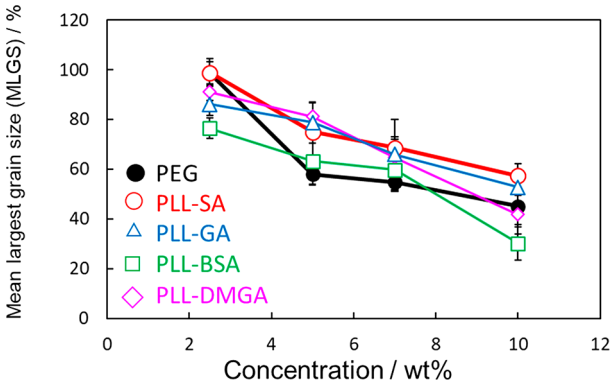


**Figure 3.** IRI activities of various polymers.

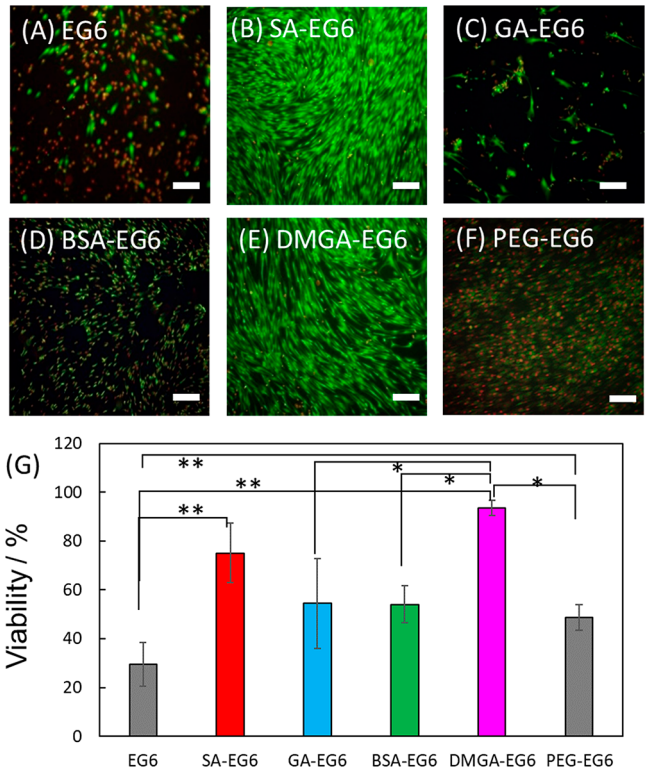


**Figure 4.** Viabilities of vitrified MSC monolayers in a −150 °C freezer using the following VSs: (A) EG6, (B) SA-EG6, (C) GA-EG6, (D) BSA-EG6, (E) DMGA-EG6, and (F) PEG-EG6. Scale bars: 100 $\mu$m. (G) Quantitative analysis of viability. *: $p < 0.05$, **: $p < 0.001$.

during cooling as DMGA-EG6. To clarify the reason for this discrepancy, cytotoxicity assays were conducted for various polyampholytes.

**Cytotoxicity.** Figure 5 shows a plot of cell viability against polyampholyte concentration. It should be noted that the viability was measured after culturing for 48 h with polymers at 37 °C and therefore does not represent the actual cytotoxicity of the polymers for vitrification because of the different conditions used (temperature and time). However, the risk of cell damage with polymers due to toxicity could be assessed using this method. From Figure 5, it can be seen that PLL-SA showed the lowest cytotoxicity, yielding around 80% viability at a polymer concentration of 8%. In contrast, PLL-BSA showed the highest cytotoxicity with viability decreasing to less than 20% at a concentration of 4%. Although PLL-DMGA showed slightly higher cytotoxicity than PLL-SA, its viability

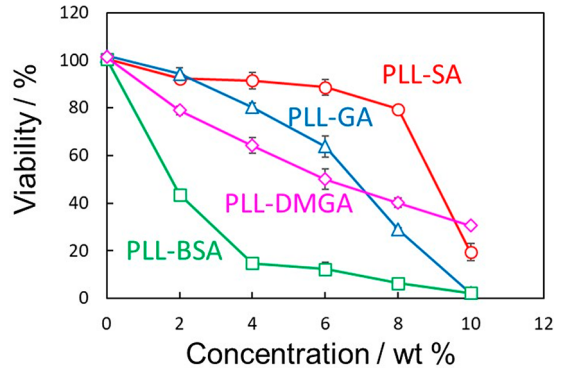


**Figure 5.** Cytotoxicities of various polyampholytes.

was highest among all the polymers when tested at a concentration of 10%. PLL-GA showed intermediate viability between those of PLL-SA and PLL-DMGA; however, a sudden decrease in viability was observed when the concentration was increased from 6%, and almost all the cells were dead at a concentration of 10%. Combining the results obtained from the cytotoxicity assays and Figure 4, it is clear that at a concentration of 10% PLL-BSA and PLL-GA caused more damage to cells than PLL-SA and PLL-DMGA. Moreover, ice crystallization damage was also inhibited when using SA and DMGA. Therefore, we used these polymers in the VSs used for the vitrification of spheroids in our further studies.

**Slow Vitrification of MSC Spheroids in a −150 °C Freezer.** Figure 6A,B shows the viabilities and recovery rates of 10 dissociated spheroids after vitrification with various VSs in a −150 °C freezer. A control sample without any vitrification solution showed a viability of almost 0%, and a positive control sample of spheroids without vitrification had a cell viability of 94.8%. Although very small differences were observed in the viabilities of polymer-containing VSs, their recovery rates showed significant differences (Figure 6B). Polyampholyte-containing VSs showed significantly higher recovery rates than those using EG6 and PEG-EG6 after warming. It was recently reported that measuring post-thaw viability can result in false positives, whereas the recovery rate represents the ratio of live cells versus the total cell number, making it a useful index for practical applications.[45] However, in our case there is the risk of underestimating the cell recovery number because of the possibility of the loss of spheroids during centrifugation and washing. Therefore, we also evaluated one of the functions of the spheroids, their fusibility.[46] The fusibilities of two spheroids were investigated for 3 days after warming; more active spheroids tend to fuse more quickly.[47] Figure 6C shows that without vitrification the spheroids fused after only 1 day, and the same fusibility was maintained in all of the spheroids vitrified with polyampholyte-containing VSs; however, in the case of spheroids vitrified with EG6 and PEG-EG6, 3 days were required for fusion. Proliferation curves of the vitrified MSC spheroids in a −150 °C freezer are shown in Figure S6. MSCs vitrified with SA-EG6 and DMGA-EG6 maintained more of their proliferation activity than those vitrified with PEG-EG6, although unfrozen cells still showed the highest growth. Furthermore, histological evaluation by HE staining was conducted to investigate the structural integrity of each cell in the spheroids. Figure S7 shows dense cell−cell adhesion in the nonvitrified spheroids. A similar integrity of cells were observed in the spheroids vitrified with polymer-containing VSs with the porous structures


https://dx.doi.org/10.1021/acs.biomac.0c00293
Biomacromolecules 2020, 21, 3017−3025

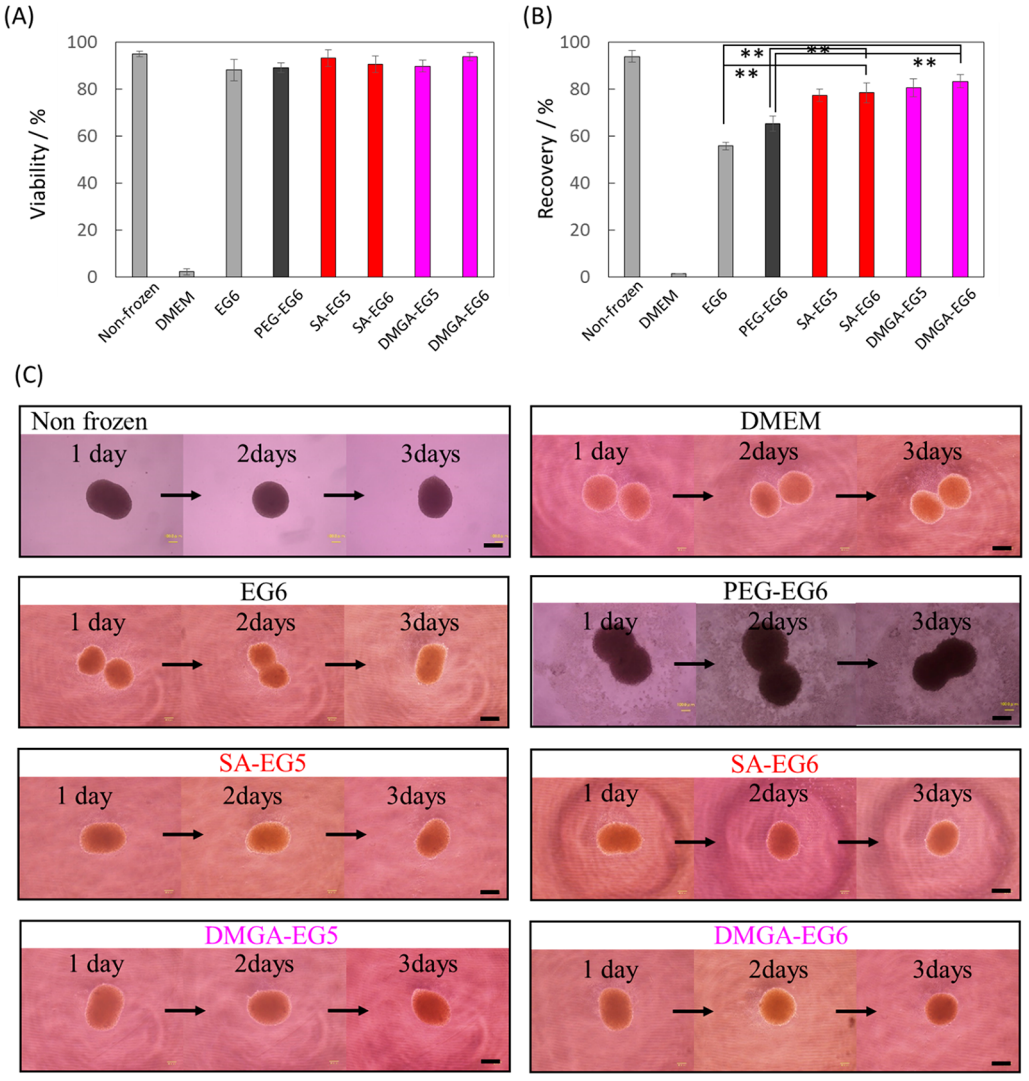


**Figure 6.** Viabilities and recovery rates of spheroids vitrified with various VSs. (A) Viabilities, (B) recovery rates, and (C) fusibilities of the vitrified spheroids. For fusibilities, two spheroids were immediately thawed and put together on a nonadhesive dish, and then their fusion was observed for 3 days. Scale bars: 200 $\mu$m.

observed being due to the formation of ice crystals and their removal after warming. This type of porous structure was also observed in EG6 samples. These results showed higher spheroid viabilities for our samples compared with the those reported for various spheroids cryopreserved with DMSO by slow freezing.[48]

It can be clearly seen from Figure 2 that the polymers inhibited ice crystallization with this inhibition increasing with the introduction of hydrophobic moieties to the molecules. Additionally, devitrification during warming could be avoided by the addition of polymers, especially those with hydrophobic side chains. However, the cytotoxicity of the polymers increased with hydrophobicity. A perfect balance was obtained in the case of DMGA-EG6, which showed the best viability for the slow vitrification of monolayers and spheroids in a −150 °C freezer. Although development of a material that can stabilize vitrification at −80 °C is ideal because −80 °C freezers are more usable, this is not easy due to the difficulty of enhancing the glass transition temperature of water. In any case, the present results indicate that spheroids, which are building blocks for tissue constructs in regenerative medicine, can be stored with high efficiency without using liquid nitrogen. This strongly suggests that a consistent automated system from culture to storage could be made.

## CONCLUSION

In this study, we developed a novel slow vitrification technique without using liquid nitrogen by using polyampholytes containing hydrophobic groups as glassy state stabilizers. The addition of PLL-DMGA into ethylene glycol-based vitrification solutions inhibited crystallization during cooling and warming at −10 °C/min, which was slower than cooling in a −150 °C freezer. PLL-DMGA possessed a lower cytotoxicity than PLL-BSA with this resulting in better monolayer vitrification properties when using PLL-DMGA in the VS. Additionally, VSs containing PLL-DMGA were able to vitrify spheroids with the highest viability and recovery while maintaining fusibility. Spheroids are building blocks for tissue-engineered constructs, and success in the cryopreservation of spheroids could open new pathways to the industrialization of tissue engineering. To build on this study, we will try to vitrify larger tissue constructs such as vessels and cartilage-like tissue without liquid nitrogen for off-the-shelf usage for clinical tissue engineering applications.


https://dx.doi.org/10.1021/acs.biomac.0c00293
Biomacromolecules 2020, 21, 3017−3025

## ■ ASSOCIATED CONTENT

### Supporting Information

The Supporting Information is available free of charge at https://pubs.acs.org/doi/10.1021/acs.biomac.0c00293.

Schematic illustrations of vitrification and warming of MSC monolayers and spheroids, $^1$H NMR spectra of the polyampholytes, viscosities of various VSs, determination of cooling speed, proliferation of MSCs after vitrification, and HE staining of spheroids (PDF)

## ■ AUTHOR INFORMATION


### Corresponding Author

**Kazuaki Matsumura** − *School of Materials Science, Japan Advanced Institute of Science and Technology, Ishikawa 923-1292, Japan;* orcid.org/0000-0001-9484-3073; Email: mkazuaki@jaist.ac.jp

### Authors

**Sho Hatakeyama** − *School of Materials Science, Japan Advanced Institute of Science and Technology, Ishikawa 923-1292, Japan*

**Toshiaki Naka** − *Shibuya Corporation, Ishikawa 920-8681, Japan*

**Hiroshi Ueda** − *Shibuya Corporation, Ishikawa 920-8681, Japan*

**Robin Rajan** − *School of Materials Science, Japan Advanced Institute of Science and Technology, Ishikawa 923-1292, Japan;* orcid.org/0000-0002-6610-9661

**Daisuke Tanaka** − *Genetic Resources Center, National Agriculture and Food Research Organization, Ibaraki 305-8602, Japan*

**Suong-Hyu Hyon** − *The Joint Graduate School of Veterinary Medicine, Kagoshima University, Kagoshima 890-8580, Japan*

Complete contact information is available at: https://pubs.acs.org/10.1021/acs.biomac.0c00293


### Author Contributions

The manuscript was written through contributions of all authors. All authors have given approval to the final version of the manuscript.


### Funding

This study was supported in part by a Grant-in-Aid, KAKENHI (25870267, 20H04532), for Scientific Research from the Japan Society for the Promotion of Science, a grant from the Canon Foundation (K11-N-028), and as a Collaborative Research Project organized by the Interuniversity Bio-Backup Project (IBBP).


### Notes

The authors declare no competing financial interest.

## ■ ACKNOWLEDGMENTS

We thank Mr. Wataru Terai and Ms. Keiko Kawamoto for critical comments and assistance in cell culture.

## ■ REFERENCES


(1) Priya, S. G.; Jungvid, H.; Kumar, A. Skin Tissue Engineering for Tissue Repair and Regeneration. *Tissue Eng., Part B* **2008**, *14* (1), 105−118.

(2) Huey, D. J.; Hu, J. C.; Athanasiou, K. A. Unlike Bone, Cartilage Regeneration Remains Elusive. *Science* **2012**, *338* (6109), 917−921.

(3) Rama, P.; Matuska, S.; Paganoni, G.; Spinelli, A.; De Luca, M.; Pellegrini, G. Limbal Stem-Cell Therapy and Long-Term Corneal Regeneration. *N. Engl. J. Med.* **2010**, *363* (2), 147−155.

(4) Rouwkema, J.; Rivron, N. C.; van Blitterswijk, C. A. Vascularization in Tissue Engineering. *Trends Biotechnol.* **2008**, *26* (8), 434−441.

(5) Mandai, M.; Watanabe, A.; Kurimoto, Y.; Hirami, Y.; Morinaga, C.; Daimon, T.; Fujihara, M.; Akimaru, H.; Sakai, N.; Shibata, Y.; Terada, M.; Nomiya, Y.; Tanishima, S.; Nakamura, M.; Kamao, H.; Sugita, S.; Onishi, A.; Ito, T.; Fujita, K.; Kawamata, S.; Go, M. J.; Shinohara, C.; Hata, K.; Sawada, M.; Yamamoto, M.; Ohta, S.; Ohara, Y.; Yoshida, K.; Kuwahara, J.; Kitano, Y.; Amano, N.; Umekage, M.; Kitaoka, F.; Tanaka, A.; Okada, C.; Takasu, N.; Ogawa, S.; Yamanaka, S.; Takahashi, M. Autologous Induced Stem-Cell−Derived Retinal Cells for Macular Degeneration. *N. Engl. J. Med.* **2017**, *376* (11), 1038−1046.

(6) Liu, B. L.; McGrath, J. J. Effects of Freezing on the Cytoskeleton, Focal Adhesions and Gap-Junctionsin Murine Osteoblast Cultures. *Conf. Proc. IEEE Eng. Med. Biol. Soc.* **2006**, 4896−4899.

(7) Meryman, H. T.; Williams, R. J.; Douglas, M. S. J. Freezing Injury from "Solution Effects" and Its Prevention by Natural or Artificial Cryoprotection. *Cryobiology* **1977**, *14* (3), 287−302.

(8) Shimizu, T.; Akahane, M.; Ueha, T.; Kido, A.; Omokawa, S.; Kobata, Y.; Murata, K.; Kawate, K.; Tanaka, Y. Osteogenesis of Cryopreserved Osteogenic Matrix Cell Sheets. *Cryobiology* **2013**, *66* (3), 326−332.

(9) Costa, P. F.; Dias, A. F.; Reis, R. L.; Gomes, M. E. Cryopreservation of Cell/Scaffold Tissue-Engineered Constructs. *Tissue Eng., Part C* **2012**, *18* (11), 852−858.

(10) Mazur, P.; Seki, S.; Pinn, I. L.; Kleinhans, F. W.; Edashige, K. Extra- and Intracellular Ice Formation in Mouse Oocytes. *Cryobiology* **2005**, *51* (1), 29−53.

(11) Mazur, P.; Koshimoto, C. Is Intracellular Ice Formation the Cause of Death of Mouse Sperm Frozen at High Cooling Rates?1. *Biol. Reprod.* **2002**, *66* (5), 1485−1490.

(12) Reubinoff, B. E.; Pera, M. F.; Vajta, G.; Trounson, A. O. Effective Cryopreservation of Human Embryonic Stem Cells by the Open Pulled Straw Vitrification Method. *Hum. Reprod.* **2001**, *16* (10), 2187−2194.

(13) Rall, W. F. Factors Affecting the Survival of Mouse Embryos Cryopreserved by Vitrification. *Cryobiology* **1987**, *24* (5), 387−402.

(14) Rajan, R.; Matsumura, K. Development and Application of Cryoprotectants. In *Survival Strategies in Extreme Cold and Desiccation: Adaptation Mechanisms and Their Applications*; Iwaya-Inoue, M., Sakurai, M., Uemura, M., Eds.; Springer Singapore: Singapore, 2018; pp 339−354.

(15) Keros, V.; Xella, S.; Hultenby, K.; Pettersson, K.; Sheikhi, M.; Volpe, A.; Hreinsson, J.; Hovatta, O. Vitrification versus Controlled-Rate Freezing in Cryopreservation of Human Ovarian Tissue. *Hum. Reprod.* **2009**, *24* (7), 1670−1683.

(16) Kuleshova, L. L.; Gouk, S. S.; Hutmacher, D. W. Vitrification as a Prospect for Cryopreservation of Tissue-Engineered Constructs. *Biomaterials* **2007**, *28* (9), 1585−1596.

(17) Katkov, I. I.; Kim, M. S.; Bajpai, R.; Altman, Y. S.; Mercola, M.; Loring, J. F.; Terskikh, A. V.; Snyder, E. Y.; Levine, F. Cryopreservation by Slow Cooling with DMSO Diminished Production of Oct-4 Pluripotency Marker in Human Embryonic Stem Cells. *Cryobiology* **2006**, *53* (2), 194−205.

(18) Yu, Z. W.; Quinn, P. J. Dimethyl Sulfoxide: A Review of Its Applications in Cell Biology. *Biosci. Rep.* **1994**, *14* (6), 259−281.

(19) Matsumura, K.; Hyon, S.-H. Polyampholytes as Low Toxic Efficient Cryoprotective Agents with Antifreeze Protein Properties. *Biomaterials* **2009**, *30* (27), 4842−4849.

(20) Rajan, R.; Hayashi, F.; Nagashima, T.; Matsumura, K. Toward a Molecular Understanding of the Mechanism of Cryopreservation by Polyampholytes: Cell Membrane Interactions and Hydrophobicity. *Biomacromolecules* **2016**, *17* (5), 1882−1893.

(21) Rajan, R.; Jain, M.; Matsumura, K. Cryoprotective Properties of Completely Synthetic Polyampholytes via Reversible Addition-Fragmentation Chain Transfer (RAFT) Polymerization and the Effects of Hydrophobicity. *J. Biomater. Sci., Polym. Ed.* **2013**, *24* (15), 1767−1780.

(22) Matsumura, K.; Bae, J. Y.; Hyon, S. H. Polyampholytes as Cryoprotective Agents for Mammalian Cell Cryopreservation. *Cell Transplant.* **2010**, *19* (6), 691−699.
(23) Matsumura, K.; Hayashi, F.; Nagashima, T.; Hyon, S. H. Long-Term Cryopreservation of Human Mesenchymal Stem Cells Using Carboxylated Poly-l-Lysine without the Addition of Proteins or Dimethyl Sulfoxide. *J. Biomater. Sci., Polym. Ed.* **2013**, *24* (12), 1484−1497.
(24) Vorontsov, D. A.; Sazaki, G.; Hyon, S.-H.; Matsumura, K.; Furukawa, Y. Antifreeze Effect of Carboxylated ε-Poly-l-Lysine on the Growth Kinetics of Ice Crystals. *J. Phys. Chem. B* **2014**, *118* (34), 10240−10249.
(25) Biggs, C. I.; Bailey, T. L.; Graham, B.; Stubbs, C.; Fayter, A.; Gibson, M. I. Polymer Mimics of Biomacromolecular Antifreezes. *Nat. Commun.* **2017**, *8*, 1546.
(26) Gibson, M. I.; Barker, C. A.; Spain, S. G.; Albertin, L.; Cameron, N. R. Inhibition of Ice Crystal Growth by Synthetic Glycopolymers: Implications for the Rational Design of Antifreeze Glycoprotein Mimics. *Biomacromolecules* **2009**, *10* (2), 328−333.
(27) Stubbs, C.; Bailey, T. L.; Murray, K.; Gibson, M. I. Polyampholytes as Emerging Macromolecular Cryoprotectants. *Biomacromolecules* **2020**, *21* (1), 7−17.
(28) Hayashi, A.; Maehara, M.; Uchikura, A.; Matsunari, H.; Matsumura, K.; Hyon, S. H.; Sato, M.; Nagashima, H. Development of an Efficient Vitrification Method for Chondrocyte Sheets for Clinical Application. *Regen. Ther.* **2020**, *14*, 215−221.
(29) Maehara, M.; Sato, M.; Watanabe, M.; Matsunari, H.; Kokubo, M.; Kanai, T.; Sato, M.; Matsumura, K.; Hyon, S.-H.; Yokoyama, M.; Mochida, J.; Nagashima, H. Development of a Novel Vitrification Method for Chondrocyte Sheets. *BMC Biotechnol.* **2013**, *13* (1), 58.
(30) Matsumura, K.; Kawamoto, K.; Takeuchi, M.; Yoshimura, S.; Tanaka, D.; Hyon, S.-H. Cryopreservation of a Two-Dimensional Monolayer Using a Slow Vitrification Method with Polyampholyte to Inhibit Ice Crystal Formation. *ACS Biomater. Sci. Eng.* **2016**, *2* (6), 1023−1029.
(31) Moldovan, N. I. Progress in Scaffold-Free Bioprinting for Cardiovascular Medicine. *J. Cell. Mol. Med.* **2018**, *22* (6), 2964−2969.
(32) Taniguchi, D.; Matsumoto, K.; Tsuchiya, T.; Machino, R.; Takeoka, Y.; Elgalad, A.; Gunge, K.; Takagi, K.; Taura, Y.; Hatachi, G.; Matsuo, N.; Yamasaki, N.; Nakayama, K.; Nagayasu, T. Scaffold-Free Trachea Regeneration by Tissue Engineering with Bio-3D Printing†. *Interact. Cardiovasc. Thorac. Surg.* **2018**, *26* (5), 745−752.
(33) Watanabe, H.; Kohaya, N.; Kamoshita, M.; Fujiwara, K.; Matsumura, K.; Hyon, S.-H.; Ito, J.; Kashiwazaki, N. Efficient Production of Live Offspring from Mouse Oocytes Vitrified with a Novel Cryoprotective Agent, Carboxylated ?-Poly-L-Lysine. *PLoS One* **2013**, *8* (12), e83613.
(34) Tsuji, Y.; Iwasaki, T.; Ogata, H.; Matsumoto, Y.; Kokeguchi, S.; Matsumura, K.; Hyon, S. H.; Shiotani, M. The Beneficial Effect of Carboxylated Poly-L-Lysine on Cryosurvival of Vitrified Early Stage Embryos. *Cryo Letters* **2017**, *38* (1), 1−6.
(35) Balcerzak, A. K.; Febbraro, M.; Ben, R. N. The Importance of Hydrophobic Moieties in Ice Recrystallization Inhibitors. *RSC Adv.* **2013**, *3* (10), 3232−3236.
(36) Deller, R. C.; Congdon, T.; Sahid, M. A.; Morgan, M.; Vatish, M.; Mitchell, D. A.; Notman, R.; Gibson, M. I. Ice Recrystallisation Inhibition by Polyols: Comparison of Molecular and Macromolecular Inhibitors and Role of Hydrophobic Units. *Biomater. Sci.* **2013**, *1* (5), 478−485.
(37) Tsutsumi, S.; Shimazu, A.; Miyazaki, K.; Pan, H.; Koike, C.; Yoshida, E.; Takagishi, K.; Kato, Y. Retention of Multilineage Differentiation Potential of Mesenchymal Cells during Proliferation in Response to FGF. *Biochem. Biophys. Res. Commun.* **2001**, *288* (2), 413−419.
(38) Gibson, M. I. Slowing the Growth of Ice with Synthetic Macromolecules: Beyond Antifreeze(Glyco) Proteins. *Polym. Chem.* **2010**, *1* (8), 1141−1152.
(39) Matsumura, K.; Bae, J. Y.; Kim, H. H.; Hyon, S. H. Effective Vitrification of Human Induced Pluripotent Stem Cells Using Carboxylated ε-Poly-l-Lysine. *Cryobiology* **2011**, *63* (2), 76−83.
(40) Zhu, S. E.; Sakurai, T.; Edashige, K.; Machida, T.; Kasai, M. Cryopreservation of Zona-Hatched Mouse Blastocysts. *Reproduction* **1996**, *107* (1), 37−42.
(41) Edashige, K.; Yamaji, Y.; Kleinhans, F. W.; Kasai, M. Artificial Expression of Aquaporin-3 Improves the Survival of Mouse Oocytes after Cryopreservation1. *Biol. Reprod.* **2003**, *68* (1), 87−94.
(42) Desbrières, J.; Martinez, C.; Rinaudo, M. Hydrophobic Derivatives of Chitosan: Characterization and Rheological Behaviour. *Int. J. Biol. Macromol.* **1996**, *19* (1), 21−28.
(43) McMillan, J. A.; Los, S. C. Vitreous Ice: Irreversible Transformations During Warm-Up. *Nature* **1965**, *206* (4986), 806−807.
(44) Deller, R. C.; Vatish, M.; Mitchell, D. A.; Gibson, M. I. Synthetic Polymers Enable Non-Vitreous Cellular Cryopreservation by Reducing Ice Crystal Growth during Thawing. *Nat. Commun.* **2014**, *5*, 3244.
(45) Murray, K. A.; Gibson, M. I. Post-Thaw Culture and Measurement of Total Cell Recovery Is Crucial in the Evaluation of New Macromolecular Cryoprotectants. *Biomacromolecules* **2020**, *21*, 2864.
(46) Arai, K.; Murata, D.; Takao, S.; Verissiomo, A. R.; Nakayama, K. Cryopreservation Method for Spheroids and Fabrication of Scaffold-Free Tubular Constructs. *PLoS One* **2020**, *15* (4), e0230428.
(47) Mironov, V.; Visconti, R. P.; Kasyanov, V.; Forgacs, G.; Drake, C. J.; Markwald, R. R. Organ Printing: Tissue Spheroids as Building Blocks. *Biomaterials* **2009**, *30* (12), 2164−2174.
(48) Ehrhart, F.; Schulz, J. C.; Katsen-Globa, A.; Shirley, S. G.; Reuter, D.; Bach, F.; Zimmermann, U.; Zimmermann, H. A Comparative Study of Freezing Single Cells and Spheroids: Towards a New Model System for Optimizing Freezing Protocols for Cryobanking of Human Tumours. *Cryobiology* **2009**, *58* (2), 119−127.


https://dx.doi.org/10.1021/acs.biomac.0c00293
*Biomacromolecules* 2020, 21, 3017−3025